Effects of Solvent Viscosity on Protein Dynamics: Infrared Vibrational Echo Experiments and Theory

K. D. Rector,[†,||] Jianwen Jiang,[‡] Mark A. Berg,[‡,§] and M. D. Fayer*[,†]

Department of Chemistry, Stanford University, Stanford, California 94305, and Department of Chemistry and Biochemistry, University of South Carolina, Columbia, South Carolina 29208

Received: July 1, 2000; In Final Form: November 8, 2000

The influence of solvent viscosity on the surface and internal structural dynamics of the protein myoglobin is studied using ultrafast infrared vibrational echo measurements of the pure dephasing of the A_1 CO stretching mode of myoglobin−CO (Mb−CO). The dephasing reflects protein structural fluctuations as sensed by the CO ligand bound at the protein's active site. Measurements made as a function of solvent viscosity at 295 K show that the pure dephasing has a marked dependence on viscosity. In addition, the pure dephasing of Mb−CO in the solvents trehalose and 50:50 ethylene glycol:water are compared as a function of temperature T (10−295 K). The pure dephasing data in the two solvents have identical $T^{1.3}$ temperature dependences at low temperatures, where both solvents are glassy solids. At higher temperatures, the Mb−CO pure dephasing has a much steeper temperature dependence in ethylene glycol:water, which is a liquid, than in trehalose, which is a glass at all temperatures studied. The steep temperature dependence in liquid ethylene glycol: water is described as a combination of a viscosity-dependent component and a temperature-dependent component. The viscosity-dependent data are analyzed using a theory that connects the fluctuations of the protein surface to the solvent's viscoelastic response. When the solvent's viscosity is lowered, the increased rate of fluctuation of the protein's surface allows more rapid internal protein dynamics, which result in more rapid dephasing. Good agreement is obtained for physically reasonable parameters. The experimental echo decay times are proportional to the cube root of the solvent viscosity $\eta^{1/3}$. This proportionality is characteristic of protein structural fluctuations that give rise to CO frequency fluctuations that are in the spectral diffusion regime (relatively slow evolution).

I. Introduction

The dynamics of proteins on a wide variety of time scales are intimately related to protein function. Fast and moderately fast fluctuations of protein structure enable a protein to sample a complex conformational energy landscape. These rapid motions give rise to the slower processes associated with protein function. Molecular dynamics simulations have shown that a protein can sample thousands of conformations on a 1−100 ps time scale.[1,2] Understanding these dynamics provides an important connection between protein function and protein structure, as determined by X-ray,[3,4] NMR,[5,6] other experimental techniques,[7−11] and theory.[1,2]

The importance of dynamic fluctuations in proteins is illustrated by myoglobin (Mb). Myoglobin is a 153-amino acid protein with the primary biological function of reversibly binding and transporting O_2 in muscle tissue. Myoglobin's ability to bind O_2 and other biologically relevant ligands, such as CO or NO, is due to a nonpeptide prosthetic group, heme, which is located in the protein's "pocket" and is covalently bound at the proximal histidine of the globin protein. The X-ray crystal structure of Mb indicates that there are no static gaps for ligands to pass through.[12−14] For ligands to move in and out of the pocket, they must traverse the intervening protein. Traversing the protein is made possible at room temperature by dynamic fluctuations in the protein structure, which open paths for ligand diffusion through the protein.[15] Because of the ability of ligands to move through the protein, in some sense, the protein has liquidlike character at room temperature.[15]

Recently, the ultrafast infrared (IR) vibrational echo technique has been applied to the study of the dynamics of myoglobin−CO (Mb−CO)[16−20] and the closely relate protein, hemoglobin−CO.[21] Vibrational echo measurements of the pure dephasing of the CO stretching mode are sensitive to the complex protein dynamics communicated to the CO ligand bound at the active site of the protein. Unlike other ultrafast techniques that involve electronic excitation of chromophores,[22,23] the vibrational echo experiments directly examine fluctuations of protein structure on the ground-state potential energy surface.

In this paper, the influence of the viscosity of the solvent on Mb−CO dynamics is examined with IR vibrational echo experiments. A study of Mb−CO in a variety of solvent mixtures at room temperature is presented. The solvents have a wide range of viscosities. These isothermal experiments demonstrate that the solvent viscosity has a significant influence on the dynamics of the protein, as sensed by the CO bound at the active site. In addition, previously reported vibrational echo pure dephasing data on Mb−CO in the solvents trehalose and a 50:50 (v:v) ethylene glycol:water mixture (hereafter referred to as EgOH) are compared over a broad temperature range.[20] The influence of the decreasing viscosity with increasing temperature in EgOH is compared to the new isothermal data. The combined data from the isothermal and temperature-dependent studies are analyzed quantitatively with a new viscoelastic theory.

In the experiments with Mb−CO in trehalose, the solvent is a glass at all temperatures studied (10−310 K). Therefore, the

[||] Present address: Bioscience Division, Los Alamos National Laboratory, Los Alamos, NM 87544.
[†] Stanford University.
[‡] University of South Carolina.
[§] Tel: (803) 777-1514.
* Corresponding author. Tel: (650) 723-4446.

10.1021/jp0023563 CCC: $20.00
Published on Web 01/16/2001

dephasing arises from the protein dynamics with a rigid, essentially infinite viscosity, solvent. In contrast, the EgOH sample has a glass transition at ~130 K and has a rapidly decreasing viscosity as temperature increases. The dephasing rates in the two solvents are identical below ~150 K, where both solvents have extremely high or infinite viscosity. In contrast, the dynamics are dramatically different above ~150 K, where the viscosities of the solvents differ substantially. With increasing temperature, the pure dephasing rate of Mb−CO in the fluid EgOH increases much more rapidly than it does in the solid trehalose. The additional dephasing in EgOH is consistent with a solvent−viscosity effect, as seen in the solvent-dependent studies. However, the viscosity of EgOH changes more than 5 orders of magnitude between 150 and 295 K, whereas the pure dephasing changes only somewhat more than 1 order of magnitude. Given the large change in viscosity and the comparatively small change in the rate of pure dephasing, the relationship between the pure dephasing and solvent viscosity is not immediately apparent.

By comparing the solvent-dependent and temperature-dependent data, we show that the change in the pure dephasing rate with temperature is caused by a combination of a viscosity dependence and a pure temperature dependence. The dephasing in glassy trehalose (infinite viscosity) is only due to pure temperature-dependent processes. When this contribution is removed from the data in fluid solvents, the remaining "reduced" dephasing rate is dependent on the viscosity of the solvent and whether the solvent viscosity is varied by changing the temperature of a single solvent or by changing the solvent composition at a fixed temperature.

A viscoelastic continuum model is presented to analyze the data. The key idea in this model is that the internal dynamics of the protein are strongly constrained by the ability of the protein's surface to move. When the protein is embedded in a disordered glass, a variety of surface topologies occur, but each protein molecule is fixed (or nearly fixed) with a single surface topology. Internal fluctuations are restricted to those protein motions that involve little motion at the surface. The vibrational echo decay time of the CO, which is sensitive to the magnitude and rate of the internal structural fluctuations of an individual protein molecule, is slow. When the protein is in a liquid, its surface can move more freely, allowing protein molecules to change their surface topologies. However, just above the glass transition temperature, the solvent is very viscous, and the surface motion is very slow. Internal dynamics connected with surface motion are also slow, and their effect on the echo decay rate remains small. Other dephasing processes that occur in the glass, i.e., the vibrational lifetime and the temperature-dependent dephasing, overwhelm the contribution of the structural fluctuations enhanced by surface motions, even though the solvent is a liquid. As the solvent viscosity is decreased further (i.e., as the temperature is raised), more rapid surface fluctuations permit faster internal protein structural fluctuations. The viscosity-dependent contribution to the echo decay becomes observable and is increasingly important as the viscosity is decreases further.

In the model, the protein is taken to be a compressible breathing sphere with surface motions that are constrained by the viscoelastic properties of the solvent. Both the magnitude and correlation time of the thermal fluctuations of the protein's size are calculated. Taking the motions of the surface to be linearly coupled to the CO frequency, we calculated the echo decay time as a function of the solvent viscosity and temperature. A detailed analysis of the properties of the echo experiment in the presence of slow modulation of the transition frequency, i.e., spectral diffusion, is essential to this model. A recent paper by us,[24] built upon earlier work,[25−29] provides the basis for the analysis. The Appendix contains an extension of this work that describes the connection between a heterogeneous distribution of spectral diffusion rates and the observed echo decay shape.

The viscoelastic model fits the data using physically reasonable parameters. The viscosity-dependent echo decay time is proportional to $\eta^{1/3}$, where η is the solvent viscosity. This behavior is characteristic of dephasing caused by spectral diffusion (relatively slowly evolving CO frequency) with an exponential frequency−frequency correlation function.[24] The entire experimental region lies within the spectral diffusion and quasistatic regions, i.e., motional narrowing of the CO vibrational line is not observed. The success of the model in describing both the isothermal (solvent-dependent) viscosity data and the temperature-dependent viscosity data supports the underlying concept that the solvent plays an important role in protein structural dynamics through its influence on protein surface motions, which in turn have a substantial affect on the internal structural dynamics of the protein.

II. Experimental Method and Procedures

A. Vibrational Echo Method. The Mb−CO absorption spectrum (1945 cm^{-1}) is inhomogeneously broadened, even at room temperature. The line shape reflects the distribution of quasistatic protein configurations that give rise to a range of CO frequencies, but the line shape provides no information about the protein dynamics. The vibrational echo is a two-pulse time domain technique that is sensitive to the dynamics of the CO frequency and can thus provide information on the protein dynamics.

In the vibrational echo experiment, two IR pulses of picosecond duration and tuned to the CO transition frequency are crossed in a sample at an angle θ with a variable time delay τ between them. The two excitation pulses interact with the sample, which then produces a third vibrational echo pulse. The vibrational echo pulse propagates along a path making an angle 2θ with respect to the first pulse. During the period between pulses, the protein dynamics cause fluctuations in the CO vibrational frequency. As τ increases, increasingly large phase errors accumulate among the CO oscillators, and the signal amplitude of the vibrational echo is reduced. A measurement of the vibrational echo intensity versus τ is an echo decay curve $S_E(\tau)$.[30,31]

For this situation, standard treatments of echo spectroscopy (or line shapes) describe two extreme limits:[30,32,33] very fast processes, which produce homogeneous dephasing and a motionally narrowed spectroscopic line, and very slow or static processes, which produce an inhomogeneously broadened spectroscopic line. In standard applications, the echo experiment extracts the homogeneous line width (dephasing rate) from a transition dominated by inhomogeneous broadening. In this case, the echo decay is given by

$$S_E(\tau) = S_E(0)\, e^{-4\tau/T_E} \qquad (1)$$

and the experimental echo decay time T_E is equal to the ensemble-averaged homogeneous dephasing time T_2 in the sense of the Bloch equations. The homogeneous line width is $(\pi T_2)^{-1}$.[30]

A common source of homogeneous dephasing is continuous frequency modulations that produce motional narrowing. For processes that cause motional narrowing, the modulation time τ_m of the fast process is fast compared to the typical size of the

frequency perturbation Δ_m (the rms range of frequencies sampled), i.e., $\Delta_m\tau_m \ll 1$.[34,35] Under these conditions, the echo measures the dephasing time $T_E^{-1} = T_2^{-1} = \Delta_m^2\tau_m$.[33] It does not measure the modulation time directly, although T_E and τ_m can be related by an appropriate model.

On the other hand, in standard treatments, the slow process is assumed to be essentially static. It has no effect on the echo decay but does contribute to the absorption line width. If the typical size of the quasistatic frequency variation is Δ_I, the Fourier transform of the absorption line shape, often called a free-induction decay, is

$$S_{FID}(\tau) = S_{FID}(0)\, e^{-\Delta_I^2\tau^2/2}\, e^{-4\tau/T_2} \quad (2)$$

If the inhomogeneous line width Δ_I is large, no information on the dephasing time or the modulation times of the system can be obtained from the line shape. However, the echo can extract the value of T_2, which is related to the system's dynamics.

The effect of the vibrational population lifetime T_1 is removed by combining the vibrational echo time T_E with a pump−probe measurement of T_1 to yield the pure echo time T_E* through

$$\frac{1}{T_E} = \frac{1}{T_E^*} + \frac{1}{2T_1} \quad (3)$$

The pure echo time T_E* is only caused by CO transition frequency fluctuations, which in turn are caused by the protein dynamics.

A variety of physical processes conform to this standard model, i.e., there is a vast separation of time scales that produces a homogeneous line (not necessarily from a motionally narrowed process) that underlies an inhomogeneously broadened absorption spectrum. Examples include absorption spectra and photon echo experiments on chromophores in low-temperature glasses,[36] where the pure dephasing is caused by two-level system dynamics,[37,38] and possibly IR absorption spectra and vibrational echo experiments on proteins at moderate to low temperatures.[20] The low-temperature and viscosity-independent processes seen in the experiments below fit this model. However as discussed below, the viscosity-dependent portion of the dephasing does not.

The standard model is adequate if the dynamics are either very fast or very slow. However, there is also a broad range of modulation times between these limits, where the echo behaves quite differently from these standard treatments. In this intermediate range, the modulation time is long enough to prevent motional narrowing, $\Delta_m\tau_m \gg 1$, but not slow enough for its effects to be eliminated from the two-pulse echo experiment. A process that occurs in this intermediate time range produces what is called spectral diffusion, i.e., relatively slow evolution of the vibrational frequency. Spectral diffusion can be studied using three-pulse stimulated echoes[30,32,33,39] or the time-dependent versions of hole burning or fluorescence line narrowing.[40,36,41] However, with proper interpretation, the two-pulse echo also becomes a powerful tool for measuring spectral diffusion.[24]

Relatively little attention has been paid to two-pulse echoes in the spectral diffusion range. Older work focused on models appropriate for spin resonance.[27−29] Following the basic results of Yan and Mukamel,[26] we have recently made a more detailed examination of the behavior of the two-pulse echo as the modulation time is varied.[24] When τ_m is in the spectral diffusion range, the echo decay time T_E is no longer equal to a dephasing time T_2 in the sense of the Bloch equations, and the interpretation of the echo time as an inverse homogeneous line width breaks down. The echo decay is more directly related to the underlying modulation time τ_m. In general, if the initial decay of the frequency−frequency correlation function has the form $1 - \tau_m^{\beta}$ (which is the short-time expansion of a variety of time-dependent functions, e.g., an exponential, a Gaussian, or a stretched exponential), then

$$\Delta_m T_E = B_\beta \Gamma\left(\frac{1}{\beta+2}\right)(\Delta_m\tau_m)^{\beta/(\beta+2)} \quad (4)$$

$$B_\beta = \frac{1}{2}\left(\frac{8}{\beta+2}\right)^{\frac{\beta+1}{\beta+2}}\left(\frac{\beta+1}{2^\beta-1}\right)^{\frac{1}{\beta+2}} \quad (5)$$

In the specific case of an exponentially decaying frequency−frequency correlation function, $\beta = 1$, and Yan and Mukamel's result is recovered[26]

$$T_E = \left(\frac{4}{3}\right)^{2/3}\Gamma(1/3)\left(\frac{\tau_m}{\Delta_m^2}\right)^{1/3} \quad (6)$$

In these equations, the standard gamma function Γ is used, and T_E is defined as the integral decay time.[24] The weak cube-root dependence, $T_E \propto \tau_m^{1/3}$, makes the echo useful over a very wide range of modulation times. It is also very different from the $T_E \propto \tau_m^{-1}$ dependence expected in the motionally narrowed limit. The data presented below on the viscosity-dependent pure dephasing of Mb−CO will be shown to follow $T_E \propto \tau_m^{1/3}$, implying that the protein structural fluctuations occur on intermediate time scales and cause viscosity-dependent spectral diffusion of the CO vibrational frequency.

A question that is not often addressed is how slow a frequency modulation needs to be before the static limit of the standard model is applicable. The answer is that there is no inherent limitation due to the modulation process itself. However, most systems have other dephasing processes that do set a limit on observing slow modulation. When the modulation is slow enough that echo decay rate predicted by eq 6 is much slower than these other dephasing processes, the modulation does not produce an observable change in the echo decay rate. The modulation can then be treated as quasistatic.

B. Experimental Procedures. The infrared vibrational echo experiments were performed at the Stanford Free Electron Laser Center. The free electron laser produces tunable, picosecond, mid-IR pulses. The experimental setup is discussed in detail elsewhere.[42,43]

The IR pulses had energies of ~0.5 μJ and were nearly transform-limited Gaussians, 1.2 ps in duration. Both the autocorrelation and the spectrum of the IR pulse were monitored continuously during the experiments. The spot size in the sample was ~100 μm. The energies at the sample in the two pulses of the echo sequence were ~50 and ~150 nJ, respectively. The vibrational lifetime T_1 was measured by pump−probe experiments (transient absorption).

The measurements were made on native horse heart myoglobin (Sigma, used without further purification). Samples were prepared by adding 15 mM of lyophilized metMb (Mb with Fe^{3+}) to either 50:50, 80:20, or 95:5% by weight glycerol:0.1 M pH 7 phosphate buffer or 50:50 v:v ethylene glycol in 0.1 M pH 7 phosphate buffer. The resulting solutions were then stirred under CO atmosphere for 8 h before being reduced by a 10 fold molar excess of dithionite.

The water sample was prepared in the same manner, except the concentration was 30 mM in 0.1 M pH 7 phosphate buffer. The trehalose sample was prepared by making a solution ~10 wt % of trehalose in 0.1 M pH 7 phosphate buffer and dissolving

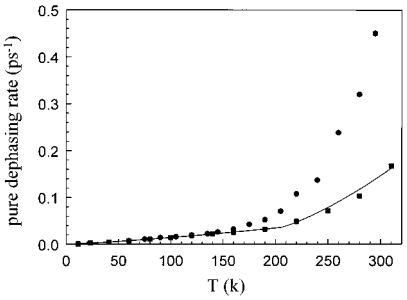

Figure 1. Temperature-dependent pure dephasing rates of Mb−CO in trehalose (■) and 50:50 ethylene glycol:water (EgOH; ●). The line through the trehalose data is the combination of eqs 8 and 9. Trehalose is a glass at all the experimental temperatures. The EgOH with protein solution goes through its glass transition at ∼140 K. The data in the two solvents are identical at low temperatures, where both solvents are glasses. Once EgOH has become a liquid, the Mb−CO pure dephasing rate increases rapidly with temperature compared to the rate measured in trehalose.

metMb in it to a final concentration of 1−2 mM. A few drops of the resulting solution were placed on a sapphire window and allowed to dry under CO atmosphere for a few days. Another sapphire window was pushed against the first one to give a thickness of approximately 100 μm.

The viscosity measurements were performed with Cannon-Ubbelohde viscometers using manufacturer's specifications. For the Mb−CO in 50:50 ethylene glycol:water temperature-dependent viscosity measurements, the viscometers were partially submerged in ice water, ethylene glycol/CO_2 (280 K, 27.7 cP), acetonitrile/CO_2 (260 K, 88.9 cP), or diethyl carbitol/CO_2 (240 K, 500 cP) mixtures. To obtain the viscosity at lower temperatures, we used a Vogel−Tamman−Fulcher equation to model the viscosity at all temperatures.[44−46] A fit was made to the measured points, along with the assumption that the viscosity is 10^{13} cP at T_g (136 K) of the solvent alone

$$\eta = (2.0 \times 10^{-4}\ \text{cP}) \exp\left(-\frac{2500\ \text{K}}{T - 70\ K}\right) \qquad (7)$$

However, a single Vogel−Tamman−Fulcher curve cannot accurately emulate the viscosity over such as large temperature range. Furthermore, T_g of the solvent plus protein will differ somewhat from the solvent alone. Therefore, the viscosities at the lowest temperatures are approximate.

III. Results

A. Temperature-Dependent Studies. Figure 1 displays the vibrational pure dephasing rates T_E^{-1} of Mb−CO in the solvents trehalose (squares) and 50:50 ethylene glycol:water (circles).[20] The glass transitions temperatures T_g of the two solvents are 353 and 136 K, respectively.[47,48] These values are for the solvents without protein in them. The glass transition temperatures of the protein/solvent mixtures should be similar to those of the pure solvents. All the temperatures included in the trehalose study are below the trehalose T_g. In EgOH, T_g occurs within the range of temperatures studied. Below T_g of the EgOH mixture, the measured values of T_E* are identical in the two solvents. For a small temperature range above the EgOH T_g, the rates remain the same. At higher temperatures, the Mb−CO pure dephasing rates in the two solvents diverge rapidly. The trehalose dephasing rate increases with temperature, but the dephasing rate in EgOH increases much more rapidly.

In the temperature range in which the two solvents are glasses, the Mb−CO pure dephasing temperature dependences are identical and independent of the solvent. (In a third solvent, 95:5 glycerol/water, the data are also identical below T_g.)[20,43] The temperature dependence in trehalose is a power law[20]

$$\frac{1}{T_E^*} = (3.5 \pm 0.1 \times 10^{-5}\ \text{K}^{-1.3}\ \text{ps}^{-1}) T^{(1.3\pm0.1)} \qquad (8)$$

up to ∼200 K (Figure 1). There is no change in the functional form near 150 K, where the data in EgOH begins to deviate markedly from the low-temperature power law (eq 8).

In trehalose, there is a change in the functional form of the temperature dependence of the pure dephasing at ∼200 K. This break in the temperature dependence may be ascribed to a dynamical transition akin to the melting of a glass as the temperature is increased.[49−56] The break in the trehalose data at ∼200 K has been discussed in detail in the context of a "protein glass transition".[20] However, the trehalose vibrational pure dephasing data alone cannot establish the existence of a protein glass transition, and the break could be caused by the onset of a separate processes.[20] Above ∼200 K, the trehalose data can be described by an Arrhenius process[20] (Figure 1)

$$\frac{1}{T_E^*(\eta=\infty, T)} = (3.3 \pm 0.2 \times 10^2\ \text{ps}^{-1}) \exp\left(\frac{-935 \pm 55\ \text{K}}{T}\right) \qquad (9)$$

Given the small number of points, the form of the data described by eq 9 cannot be considered definitive. The data can also be fit well with a Vogel−Tamman−Fulcher (VTF) temperature dependence.[44−46] The Arrhenius and the VTF functional forms are indistinguishable below the denaturation temperature of the protein. Regardless of the exact functional form above ∼200 K, it is clear that there is a change in the temperature dependence near 200 K. Since trehalose is a glass well above 200 K, the change in the temperature dependence does not arise from a change in the solvent viscosity.

In considering the origin of the difference in the temperature dependences in the two solvents, we can be confident that the CO pure dephasing is not caused by direct interaction with the solvent. Rather, the vibrational dephasing is caused by protein structural fluctuations.[17,18,43] The identical power law temperature dependence in the two solvents seen in Figure 1 (and a third solvent[20,43] not shown), i.e., the same slopes and the same values of the pure dephasing, shows that the dephasing is not affected by the specific chemical composition of the solvent. This fact is one clear demonstration that the solvent does not directly interact with the CO to produce pure dephasing.

The manner in which the Mb protein fluctuations are communicated to the CO bound at the active site and produce pure dephasing has been discussed previously.[17,18,43] On the basis of mutant Mb−CO pure dephasing studies,[17,18] a model was developed that ascribes the CO vibrational pure dephasing to global structural fluctuations of the protein. The protein structural dynamics produce fluctuating electric fields that cause the CO vibrational frequency to fluctuate via the Stark effect. However, in the mechanism proposed previously, the fluctuating electric fields were thought to produce changes in the CO frequency by changing the extent of back-bonding from the heme macrocycle to the CO π* antibonding orbital. While changes in the electric field do produce changes in back-bonding, this is not the cause of the CO frequency shifts.[57,58] A number of detailed quantum chemical studies[57,58] and experimental studies[59] demonstrate that changes in the electric field act directly on the CO, changing its frequency through the Stark effect. The theoretical and experimental studies are for static changes in the electric field,[57−59] whereas the pure dephasing

TABLE 1: Viscosity and Temperature-Dependent Echo Dephasing Rates of Mb−CO

solvent	temp. (K)	viscosity[b] (cP)	pure dephasing rate (ps^{-1})	reduced pure dephasing rate (ps^{-1})
H_2O	295	8.5	0.67 ± 0.05	0.53 ± 0.06
50:50 EgOH:H_2O	295	14	0.45 ± 0.02	0.32 ± 0.02
50:50 GOH:H_2O	295	50	0.31 ± 0.01	0.17 ± 0.01
80:20 GOH:H_2O	295	400	0.25 ± 0.01	0.11 ± 0.01
95:5 GOH:H_2O	295	2300	0.24 ± 0.01	0.10 ± 0.01
trehalose	295	n.a.	0.14 ± 0.005	n.a.
50:50 EgOH:H_2O	295	14	0.45 ± 0.02	0.31 ± 0.02
50:50 EgOH:H_2O	280	30	0.32 ± 0.01	0.21 ± 0.01
50:50 EgOH:H_2O	260	100	0.24 ± 0.01	0.15 ± 0.01
50:50 EgOH:H_2O	240	480	0.14 ± 0.005	0.070 ± 0.005
50:50 EgOH:H_2O	220	(3500)	0.11 ± 0.005	0.060 ± 0.005
50:50 EgOH:H_2O	205	(22,000)	0.070 ± 0.002	0.036 ± 0.002
50:50 EgOH:H_2O	190	(220,000)	0.052 ± 0.002	0.020 ± 0.002

[a] Listed are the solvent composition, temperature, viscosity, measured pure dephasing rates (eq 3), and reduced dephasing rate (eqs 8−10). Values in parentheses are extrapolated using eq 7. [b] The error range of the temperature-dependent viscosity measurements below room temperature is ∼10%. The error range for the lowest three temperatures given in parentheses is estimated at 20%. The error range on the room temperature measurements is approximately ∼3%. n.a. stands for not applicable.

is caused by time-dependent electric fields that arise from the protein's structural dynamics. In either case, the Stark effect is the primary mechanism causing frequency shifts in the CO vibration.

It is noted that the mechanism proposed to explain the relationship of the vibrational lifetime T_1 of CO in heme proteins and heme model compounds[60−62] still holds. Vibrational relaxation requires a bath to take up the energy of the relaxing mode. The large density of high-frequency modes of the heme provides the bath, and the coupling is via the π back-bonding interactions of the CO with the heme. The linear correlation observed between the shift in vibrational frequency and the change in the vibrational lifetime[60−62] from one molecule to another can be caused by a change in electric field that changes both the frequency of the vibration and the back-bonding. Changing the back-bonding alters the coupling of the CO to the heme, modifying the vibrational lifetime.

Given that the CO does not directly interact with the solvent, an indirect explanation must be found for the differences in dephasing in the two solvents. These differences occur at temperatures above ∼150 K (Figure 1). Above this temperature, the major difference between Mb−CO in trehalose and Mb−CO in EgOH is that trehalose is a glass and EgOH is a liquid. As the temperature of the EgOH sample is increased above the solvent T_g, the viscosity of the liquid drops very rapidly. An obvious question is whether the change in viscosity of the solvent can influence the protein structural fluctuations that cause pure dephasing. Is the temperature dependence observed above ∼150 K in EgOH really a combined temperature and viscosity dependence? Frauenfelder and co-workers have shown that the four potential barriers a CO ligand must overcome to bind to Mb are dependent upon solvent viscosity.[15] Other solvent parameters, such as pH, ionic strength, thermal conductivity, permittivity, and dielectric constant affect these barriers to a much lesser extent.[15] The protein motions responsible for CO barrier crossing are sensitive to changes in viscosity because the protein barriers are dynamic in nature and are influenced by thermal structural fluctuations of the protein.[63]

B. Isothermal Studies. To determine if solvent viscosity plays a role in the temperature-dependent Mb−CO data in EgOH pure dephasing, we measured the isothermal (295 K) viscosity dependence. Mb−CO samples were prepared in a variety of solvents of varying viscosity at room temperature, and the vibrational echo response was recorded.

For the isothermal viscosity data, the instrument response time was on the same order as the sample dephasing time. To extract

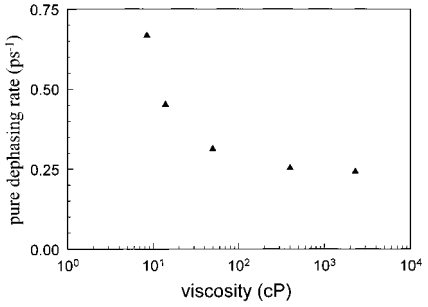

Figure 2. Isothermal (295 K) viscosity-dependent pure dephasing rates in solvents of varying composition (see Table 1). The data demonstrate that the Mb−CO pure dephasing has a significant dependence on viscosity at constant temperature.

T_E*, the τ-dependent echo signal was fit by numerically evaluating all of the rephasing and nonrephasing third-order nonlinear polarization terms (diagrams) that contribute to the signal in the vibrational echo wave-vector-matched direction.[39] Because the echo decay shapes at all lower temperatures are close to exponential, we also modeled the echo time dependence at room temperature as exponential. The details of these types of calculations are presented elsewhere.[64] At room temperature, the vibrational pure dephasing is the overwhelmingly dominant contribution to the echo decay; the lifetime contribution is negligible. Therefore, for the room temperature isothermal viscosity data, only vibrational echo experiments were performed; the corresponding pump−probe measurements of T_1 and the correction of eq 3 were unnecessary.

The measured dephasing rates for each sample at room temperature and the corresponding viscosities are listed in Table 1 and shown in Figure 2. Figure 2 demonstrates that the Mb−CO pure dephasing has a significant dependence on viscosity at constant temperature. Therefore, it is reasonable to consider the temperature-dependent difference between the EgOH data and the trehalose data shown in Figure 1 as arising from the temperature dependence of the EgOH viscosity rather than a direct temperature effect. We hypothesize that the Mb−CO pure dephasing rate in EgOH is a combination of a direct temperature dependence, as seen in the trehalose data, and an additional contribution that is dependent on the viscosity of the solvent.

We wish to quantify the influence of changing viscosity on the pure dephasing. At room temperature, the trehalose sample displays significant pure dephasing although the viscosity is essentially infinite. Thus, the pure dephasing rate in trehalose represents the infinite viscosity point. The pure dephasing in

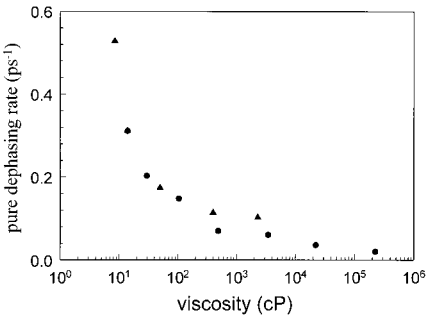

Figure 3. Triangles are the isothermal (295 K) viscosity-dependent Mb−CO reduced pure dephasing rates. The data are the pure dephasing rates at a given viscosity minus the 295 K rate at infinite viscosity (eq 10). The circles are the temperature-dependent Mb−CO in 50:50 ethylene glycol:water (EgOH) pure dephasing rates minus the corresponding infinite viscosity (trehalose data) pure dephasing rates at each temperature plotted against the viscosity of the EgOH protein solution for each temperature. The circles are the viscosity-induced part of the pure dephasing rate at various temperatures. (Note that the point at ~10 cP is an overlapping circle and triangle.) The fact that the circles and the triangles are intermixed demonstrates that the viscosity component and the temperature component of the pure dephasing rates are additive, within experimental error.

this sample is only due to temperature-induced structural fluctuations of the protein that do not require participation of solvent motion to any significant extent. To obtain the viscosity dependence, we subtracted the room-temperature infinite viscosity pure dephasing rate, i.e., the rate in trehalose, from the pure dephasing rates measured at finite viscosities

$$\frac{1}{T_E^r(\eta)} = \frac{1}{T_E(\eta,T)} - \frac{1}{T_E(\eta=\infty,T)} \tag{10}$$

T_E^r is the reduced pure dephasing time.

The model reflected in eq 10 takes the temperature-dependent contribution to the pure dephasing at infinite viscosity and the viscosity-dependent contribution to be additive. The additivity feature of the model can be tested experimentally. Figure 3 is a plot of the reduced isothermal viscosity-dependent data from Figure 2 (triangles). These data were taken as a function of viscosity at room temperature. The room-temperature infinite viscosity pure dephasing rate was subtracted off using eq 10. The circles in Figure 3 are obtained from the temperature-dependent EgOH data of Figure 1. For each EgOH point, the pure dephasing rate in trehalose (eqs 8 and 9) was subtracted off. For the points between room temperature and 210 K, the viscosity is known, and the difference between the EgOH data and the trehalose data are plotted at the appropriate viscosity. Notice that within experimental error, the isothermal viscosity points (triangles) and the viscosity points obtained at various temperatures (circles) are intermingled. The trend is the same. Therefore, the infinite viscosity pure dephasing rate and the viscosity-dependent pure dephasing rate are additive within experimental error.

IV. Viscoelastic Theory of the Viscosity Contribution to Pure Dephasing

The experimental data presented above have isolated a viscosity-dependent dephasing process with two qualitative features that require explanation. First, the reduced dephasing rate is almost entirely determined by the solvent viscosity. The detailed chemical properties of the solvent do not make much difference, as shown by the isothermal data taken in a variety of solvents (Figure 2). The apparent difference in the temperature dependence between EgOH and trehalose (Figure 1) is almost entirely caused by the temperature dependence of the viscosity (Figure 3). The fact that the CO pure dephasing has a strong sensitivity to the solvent viscosity might at first seem puzzling. The CO is located internally in myoglobin, precluding a direct interaction between the CO and the bulk solvent. The dephasing is not sensitive to the particular solvent when the solvents are all glasses. The frequency of the Mb−CO stretch is insensitive to the solvent, again demonstrating that there is no direct interaction of the solvent with the CO.

The second experimental result is that the viscosity dependence of the dephasing rate is relatively weak. The data summarized in Figure 3 cover changes of viscosity of more than five orders-of-magnitude, but the reduced dephasing rate changes by only about $1^1/_2$ orders of magnitude.

These facts can be explained using the following model. Due to a vibrational Stark shift, the change in the frequency of the CO ω is directly proportional to the electric field E at the CO's site.[59] Fluctuations in the instantaneous configuration of the protein cause fluctuations in this electric field δE. If $\omega°$ is taken as the frequency at the time-averaged protein configuration, the time-dependent CO frequency is

$$\omega(t) = \omega° + \frac{\delta\mu_{01}\,\delta E(t)}{\hbar} \tag{11}$$

The value of the change in dipole moment from the ground to first excited vibrational level, $\delta\mu_{01} = 0.14$ D $= 2.4$ cm^{-1}/(MV/cm), has been measured recently.[59] When the protein is in a solid, glassy solvent, the surface topology of the protein is essentially fixed. The solvent resists any shearing motions, so the surface of the protein can only change by elastic distortions of the glassy solvent. Because the compressibility of a glass is very small, surface motions of the protein are severely limited. If the internal motions of the protein are strongly coupled to motion of the surface, the internal protein dynamics are also tightly constrained. The protein can still undergo internal structural fluctuations, but only those fluctuations are permitted that do not move the protein's surface very far. These motions, as sensed by CO bound at the active site of Mb, are reflected in the temperature-dependent pure dephasing measured in trehalose. The only feature of the solvent that is important is that it keeps the protein surface fixed. Thus, in EgOH below its T_g, the behavior of Mb−CO is identical to its behavior in trehalose. The pure dephasing of Mb−CO in glycerol/H_2O is also identical at temperatures below that of the solvent's glass transition.[20]

As the temperature is increased above T_g, a new contribution to the Mb−CO echo decay measurements comes into play. When the solvent is a fluid, the range of motion of the protein's surface, and, as a result, the range of its internal motions, is much greater. The additional amplitude of the protein motion increases the magnitude of dynamic fluctuations in the electric field at the CO bound in the interior of the protein and, thus, in the magnitude of dynamic fluctuations in the CO vibrational frequency. However, the viscosity of the solvent determines the rate of this increased motion. Just above T_g, the liquid is extremely viscous, and the increased protein motions are very slow. The effect on the CO echo decay is correspondingly weak. The increased dephasing caused by motions allowed by the solvent is undetectable over the background dephasing rate produced by the solvent-independent processes. In other words, just above T_g, the solvent-induced dephasing is still in the quasistatic limit and is eliminated by the echo experiment. In

EgOH, this case applies from ~136−150 K. The dephasing rate remains almost identical to that in the true glass, trehalose (Figure 1).

As the temperature is increased further, the viscosity of the solvent drops rapidly. At some point, the solvent-dependent protein structural fluctuations become fast enough to have a measurable contribution to the echo decay. The system enters the spectral diffusion regime. Further increases in temperature reduce the solvent viscosity and increase the internal protein fluctuation rate by many orders of magnitude. The echo decay rate also increases. However, because of the weak power law connecting the fluctuation time and the echo decay time in the spectral diffusion region (eq 6), the echo decay rate only increases weakly with decreasing viscosity, a little over 1 order of magnitude. This region covers ~150−295 K in EgOH (Figure 1).

At a low enough solvent viscosity, the fluctuations would be fast enough that the fluctuations would change from spectral diffusion to motionally narrowed dephasing. In the Mb−CO system, this change lies above the temperature range examined in these experiments. Most likely, this region cannot be reached in Mb without denaturing the protein.

The model gives a good qualitative account of the dephasing rate versus temperature in EgOH and in trehalose. Moreover, it explains how the CO vibration can be sensitive to the solvent viscosity without any direct coupling between the solvent and the CO. The disparity in the magnitude of change in the viscosity and the echo decay rate is also accounted for.

To quantify this model, we will extend a recent viscoelastic continuum theory of solvent dynamics. This theory has been used to calculate time-dependent electronic solvation dynamics as well as vibrational absorption line shapes.[65−68] The theory has had considerable success in reproducing important features of these experiments.

We model the protein as a sphere of radius r_p embedded in a viscoelastic and continuous solvent. The solvent's viscoelastic behavior is characterized by a decaying shear modulus $G(t)$. For sufficiently short periods, the solvent behaves as a solid with a short-time (infinite-frequency) shear modulus G_∞. The relaxation of the solvent's bulk modulus K_∞ is ignored. Its relaxation typically involves less than 20% of its total magnitude, and even this small effect only comes in due to deviations from spherical symmetry. At times comparable to or longer than the decay time of $G(t)$, the solvent can flow, allowing additional fluctuation of the protein's surface. This decay time is directly related to the solvent viscosity. The protein is also treated as a continuous material with a bulk modulus K_p.

In general, two time scales for motion are possible in this model. Rapid elastic waves (inertial motion) propagate through the system in times that are governed by the infinite-frequency moduli and are generally well under 1 ps. These motions are not normally effective in causing dephasing[65] and are ignored here. The slower time scale is governed by the relaxation of $G(t)$ (structural or diffusive motion). We assume that there is a good separation between this time scale and both the inertial motions and any relaxation of the protein properties. The separation of inertial and diffusive times usually occurs for viscosities above 1 cP,[66] so the assumption is easily satisfied in the current experiments. Viscous relaxation or "flow" of the protein in response to its distortion are ignored. With these assumptions, the protein will transmit changes in its surface to its interior almost instantaneously.

Before continuing, we can pause to consider the separability of the viscosity-dependent and viscosity-independent processes found experimentally (eq 10 and Figure 3). In our model, we assume that the corresponding protein motions with a frozen surface and the additional motion allowed by moving the surface can be treated as independent processes. We do not assume that these two types of motion involve different protein coordinates. Both processes may involve the same internal motions of the protein. The freeing of the surface only increases the amplitude of the motion along the same coordinates that cause the viscosity-independent dephasing. The independence of the frozen-surface dynamics from the free-surface dynamics is justified by the assumption we just made concerning a separation of time scales between the internal protein dynamics and the viscous flow of the solvent. Any internal equilibration of the protein is assumed to be much faster than the viscous relaxation of shear stress in the solvent. As a result, information about the state of the surface is transmitted rapidly throughout the protein. It is also possible that the protein has conformational changes that relax much more slowly than the solvent. Any change in the CO frequency due to these conformations will be in the quasistatic limit and does not contribute to the echo decay.

With this separation of time scales, the additivity of the viscosity-dependent and viscosity-independent dephasing rates is justified. The viscoelastic model only treats the viscosity-dependent dephasing reflected in the reduced dephasing time $T_E^r(\eta)$.

We only allow spherical fluctuation in the protein's volume; i.e., it is treated as a breathing sphere. More complex shape fluctuations are certainly possible, but their behavior is very similar to the behavior of spherical fluctuations.[66] For simplicity, only the spherical fluctuations are included here.

With this simplification, the protein's fluctuations are fully characterized by its change in radius δr_p. These changes in radius are linked to changes in the electric field at the CO due to displacement of charged groups within the protein. We do not attempt to treat the details of this coupling but only introduce a phenomenological proportionality constant b

$$\delta E(t) = b\delta r_p(t) \tag{12}$$

The viscosity-dependent protein dynamics in our model are now isomorphic to the structural dynamics in our other viscoelastic models.[65−67] The magnitude of the thermal fluctuations in the protein radius is

$$\langle \delta r_p^{\,2} \rangle = \frac{kT}{12\pi K_p r_p} \tag{13}$$

where k is the Boltzmann constant. Combining eqs 11, 12, and 13, we find the magnitude of the CO frequency modulation to be

$$\Delta_m = \langle (\omega(0) - \omega^\circ)^2 \rangle^{1/2} = \frac{b\delta\mu}{h\sqrt{4\pi}} \left(\frac{kT}{3K_p r_p} \right)^{1/2} = \Delta_0 \left(\frac{T}{T_0} \right)^{1/2} \tag{14}$$

where $\omega(0)$ is the frequency at $t = 0$. The most important feature of eq 14 is the temperature dependence of Δ_m. The temperature independent constants are collected into Δ_0, the modulation amplitude at the reference temperature T_0. In this paper, we will use $T_0 = 295$ K. (We are only concerned with the portion of the frequency shift that relaxes on the structural time scale, i.e., $\Delta_m = f^{1/2}\Delta$ in the notation of ref 63.)

The relaxation time of the thermal fluctuations is proportional to the solvent viscosity, with the proportionality constant determined by the solvent and protein moduli

$$\tau_m = \alpha \frac{\eta}{G_\infty} \tag{15}$$

$$\alpha = 1 + \frac{4G_\infty}{3K_p} \tag{16}$$

As an estimate, we can assume $K_p \approx K_\infty$ and take the Cauchy relation for simple solids,[69] $G_\infty = (^3/_5)K_\infty$, giving $\alpha \approx {}^9/_5$. On the basis of the value for water,[70] we initially estimate $G_\infty \approx 10 \times 10^{10}$ dyn/cm^2 for our solvents. Over the experimental range of viscosities of roughly $10-10^6$ cP, modulation times in the approximate range of 2 ps−200 ns are expected.

With eqs 14−16 from the viscoelastic model, the echo response can be calculated under a wide variety of conditions. Given the long modulation times predicted, we first assume that the fluctuations are in the spectral diffusion regime, $\tau_m \Delta_m \gg 1$. From eqs 4, 5, 14, and 15

$$T_E \sqrt{\frac{T}{T_0}} = C\left(\eta(T)\sqrt{\frac{T}{T_0}}\right)^{\frac{\beta}{\beta+2}} \tag{17}$$

$$C = B_\beta \Gamma\left(\frac{1}{\beta+2}\right)\left(\frac{\alpha^\beta}{G_\infty^\beta \Delta_0^2}\right)^{\frac{1}{\beta+2}} \tag{18}$$

The dominant source of temperature dependence in eq 17 is the viscosity, which has a steep VFT dependence on temperature. All the constants in eq 18 can be reasonably approximated as temperature-independent. The moduli are actually temperature-dependent, but this dependence is relatively weak.[71] The explicit temperature factors in eq 17 are also weak, going as the square root of the temperature.

Thus, the viscoelastic theory explains why the solvent viscosity is the dominant factor in determining the dephasing rate. Moreover, for reasonable values of β, i.e., near unity, the dephasing rate varies with the viscosity raised to a small fractional power. Again, the theory is in accord with the relatively weak dependence on viscosity observed in the experiments.

The viscoelastic theory is tested quantitatively in Figures 4 and 5. First, consider Figure 4. Both the isothermal and temperature-dependent data are included. Equation 17 predicts a linear relationship on this log plot with a positive slope. If the system were in the fast modulation limit, the slope would be negative, and if there were a shift between these limits as the viscosity changed, there would be a turn around in the slope and a minimum in the curve.[24] No such turnaround is seen in the data, so our assumption that the system is in the spectral diffusion regime is valid.

The line in Figure 4 shows a line with the slope predicted by eq 17 for $\beta = 1$, which corresponds to a cube-root dependence of the dephasing rate on the viscosity. This line is a good description of the data. The points at the highest viscosities fall off the line, but these are the points with the greatest uncertainty in the viscosities. $\beta = 1$ corresponds to an exponential decay of the CO frequency−frequency correlation function and, consequently, of the solvent shear modulus.[24] It is common for relaxation functions to become nonexponential at high viscosity, which would lead to a smaller value of β. This effect could also contribute to the deviations seen at the highest viscosities.

The solid line in Figure 5 displays the fit of the reduced dephasing rate from Figure 4, combined with the trehalose dephasing data through eq 10, to recreate the full temperature/viscosity-dependent dephasing rate in EgOH. The theory does

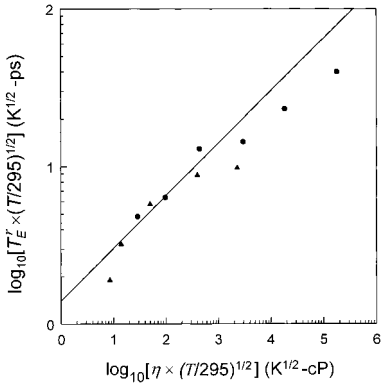

Figure 4. Reduced echo pure dephasing time from both the isothermal (▲) and temperature-dependent (●) measurements are plotted against viscosity as indicated by eq 17. Both the dephasing time and viscosity are corrected for the temperature. The line corresponds to the cube-root dependence on viscosity predicted for an exponentially relaxing shear modulus ($\beta = 1$). The line also corresponds to the fit shown in Figure 5.

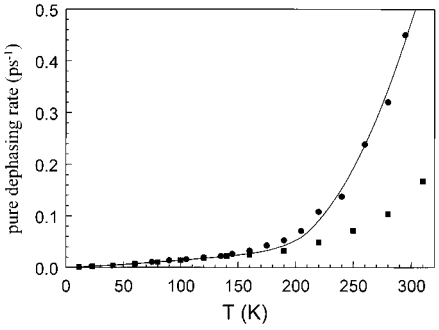

Figure 5. Temperature-dependent Mb−CO pure dephasing rates in trehalose (■) and in 50:50 ethylene glycol:water (EgOH; ●) from Figure 1. The line through the EgOH data is the fit to the viscoelastic theory (eq 17) added to the temperature dependence in trehalose (see also Figure 4). The viscoelastic theory attributes the difference between the trehalose (■) and EgOH (●) rates to fluctuations of the protein surface that are governed by the solvent viscosity. The theory does a remarkable job of reproducing the data.

a remarkable job of reproducing the data qualitatively and almost quantitatively. It misses at the lowest temperatures for the same reasons as just discussed. The calculated curves in Figures 4 and 5 are different methods of comparing theory and experiment.

Fits were also performed using the full integrals for the vibrational echo response.[24] This numerical procedure does not limit the calculations to the spectral diffusion regime, and if it were possible to fit the data in the motional narrowing regime, such fits would emerge from the calculations. The viscoelastic model provided the forms of the modulation time and magnitude of the solvent-induced fluctuations; the absorption line width was taken as the width of an additional inhomogeneous broadening process. The full vibrational echo calculations produced fits that are essentially the same as those shown in Figures 4 and 5. This result confirms that motional narrowing effects are not important, even at the lowest viscosities examined.

The fit of the theory to the data involves only one adjustable parameter C (eq 18). The fit gave $C = 1.4$ ps/cP$^{1/3}$. We cannot make an estimate of this parameter because the magnitude of b in eq 12 is not independently known. On the other hand, using eqs 14 and 18, we can find the value of b corresponding to our fit. With $\delta\mu_{01} = 0.14$ D, an average protein radius of 3.5 nm and our previous estimate $\alpha \approx {}^9/_5$, we find $b \approx 8.3 \times 10^3$ dyne esu^{-1} cm^{-1}.

The fit value of C can be used to place a bound on Δ_0. For the spectral diffusion limit to hold, $\Delta_m\tau_m \geq 1$.[24] Combining this condition with eqs 14 and 18 yields the condition

$$\Delta_0 > \frac{\left(\frac{4}{3}\right)^2\Gamma\left(\frac{1}{3}\right)}{C}\left[\frac{3}{\eta}\left(\frac{T_0}{T}\right)^{1/2}\right]_{min}^{1/3} = 1.1\ ps^{-1} \qquad (19)$$

The quantity in the square brackets is evaluated at the lowest viscosity used in the fit (8.5 cP).

Another bound can be placed on Δ_0 by using the observed IR absorption line width, which is 15 cm^{-1} fwhm at room temperature, or $\Delta_I = 1.2\ ps^{-1}$ (see eq 2). Because the solvent-induced frequency modulation is in the spectral diffusion limit, its contribution to the absorption line width is the full value of Δ_m. Thus, $\Delta_m \leq \Delta_I$, or $\Delta_I \leq 1.2\ ps^{-1}$.

Combining these two limits gives $1.1\ ps^{-1} \leq \Delta_0 \leq 1.2\ ps^{-1} = \Delta_I$. In other words, the process responsible for the viscosity-dependent spectral diffusion must account for almost all of the IR line width. If this were not true, this process would become motionally narrowed at low viscosity and a turn over would be seen in Figure 4.

If $\Delta_0 \approx \Delta_I$ is taken account along with eq 18, our previous estimate of $\alpha \approx {}^9/_5$ and the measured value of C gives a value for the solvent shear modulus $G_\infty = 15 \times 10^{10}$ dyn/cm^2. For comparison, the value for pure water is $G_\infty = 11 \times 10^{10}$ dyn/cm^2.[70] Given the errors in the experimental fit and in the estimated parameters, the inferred value of G_∞ is very reasonable. (Implicit in our analysis is an assumption that the value of this modulus is independent of solvent composition and temperature. Errors in this approximation presumably lead to some of the scatters around the fit.) The fit value of G_∞ then leads to an estimate of the protein modulation time in the various solvents through eq 15, $\tau_m \approx (0.12\ ps/cP)\ \eta$.

A number of imprecisely known factors contribute to a moderate level of uncertainty in all of the above estimates. However, they should be accurate enough to establish the approximate magnitude of the parameters involved in solvent-induced protein dynamics. The fact that all these numbers are internally self-consistent as well as compatible with our a priori physical expectations is reassuring.

Another clear experimental result is that the viscosity-dependent dephasing in EgOH is active at temperatures below the putative protein glass transition (Figure 1). The Mb−CO pure dephasing data in trehalose has a break at ~200 K that may be caused by this transition.[20] A large quantity of other experimental data indicates a transition around the same temperature;[49−56] therefore, it may be reasonable to assume that the break in the trehalose data does arise from a dynamical transition of the protein. Although the viscosity-independent dephasing processes in trehalose do show a break at this transition, the additional viscosity-dependent dephasing EgOH does not show an observable break at the protein glass transition.

This result is entirely compatible with the viscoelastic theory. Within this theory, the response of the solvent is governed by its shear relaxation, but the protein only responds through its compressibility.[72] For typical liquids, the compressibility only changes ~20% at the glass transition.[73,74] If the change in protein compressibility at the protein glass transition is similarly small, then no observable break in the internal dynamics connected with surface motion would be expected. This conclusion is supported by computer simulations, which have shown there is not a dramatic change in Mb's dynamical behavior across the protein glass transition.[1,2] Thus, the viscoelastic theory predicts that the viscosity-dependent dephasing mechanism should remain active below the protein glass transition, as is observed experimentally. In general, the solvent viscosity can influence a protein's dynamics even below its glass transition.

Another possible reason that viscosity-dependent pure dephasing in EgOH is observed below 200 K is a shift in the protein glass transition to lower temperature in the liquid solvent.[20] This idea is supported by the fact that in a system with a large surface-to-volume ratio in which the surface is free to move, such as a thin polymer film, the glass transition temperature shifts to a lower temperature than that of the bulk material.[75] The protein has a large surface-to-volume ratio, and in the liquid, the surface is free to move. Either of the explanations given above or a combination of them could be responsible for the viscosity dependence of the Mb−CO pure dephasing in EgOH at temperatures below 200 K, the temperature of the protein glass transition in the trehalose solid solvent.

For a spectral diffusion process with an exponential frequency−frequency correlation function, the decay of the echo signal $S_E(\tau)$ is predicted to be distinctly nonexponential.[24] This result is in apparent contradiction to the experimental finding of nearly exponential echo decays. However, the highly nonexponential decay function was derived assuming homogeneous kinetics. As the Appendix discusses in detail, heterogeneous kinetics can give rise to the observed decay shapes for a spectral diffusion process. The analysis presented above is not changed in a substantive way if the echo decay and modulation times used above are identified with the average values of the corresponding distributions.

V. Concluding Remarks

The viscoelastic theory is able to reproduce the fundamental nature of the vibrational echo pure dephasing data's temperature dependence and the isothermal viscosity dependence. The agreement between theory and experiment supports the physical model presented above for the role that surface fluctuations play in structural dynamics of a protein. Protein surface fluctuations are dependent on the viscoelastic properties of the solvent. Thus, the dynamics of a protein are intimately coupled to the dynamical properties of the medium in which it is embedded.

The temperature-dependent Mb−CO in EgOH pure dephasing is really a combination of a temperature dependence and a viscosity dependence. As the viscosity of the solvent is reduced, the surface becomes increasingly free to fluctuate, permitting protein structural fluctuations that are not possible when the proteins surface topology is fixed by a glassy solvent. The viscoelastic model is supported by the agreement between theory and temperature-dependent experiments in Figure 5 and with the combined temperature-dependent and isothermal viscosity-dependent data and theory in Figure 4. The results also suggest that the addition of structural fluctuations that involve the surface do not substantially change the temperature dependence of the structural fluctuations that occur in the absence of surface motions. Motions of the solvent enable the surface fluctuations. Recent computer simulations have addressed the importance of solvent dynamics in protein structural fluctuations.[2]

The work presented above establishes the connection between solvent viscosity, surface fluctuations, and Mb−CO vibrational pure dephasing measured by ultrafast vibrational echo experiments. The Mb−CO vibrational pure dephasing provides an observable sensitive to the global structural fluctuations of the protein. The data show that the Mb−CO viscosity-dependent dephasing is neither in the fast modulation (motional narrowing) regime nor in the static inhomogeneous limit. The recent theoretical developments that describe the vibrational echo

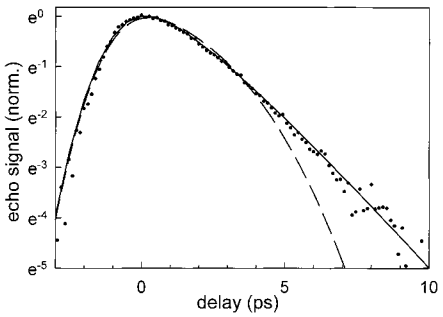

Figure 6. Shape of the echo signal at 220 K as a function of pulse delay (●) is apparently exponential, whereas the decay shape (dashed curve) predicted for spectral diffusion in a system with homogeneous kinetics with an exponential decay of the frequency−frequency correlation function (eq A2) is strongly curved on this semilog plot. A spectral diffusion model including heterogeneous kinetics produces a decay shape (solid curve) very close to the data. Heterogeneous kinetics changes the shape of the vibrational echo decay but does not change the calculated viscosity or temperature dependence of the average decay rate.

experiment and other echo experiments in the regime of intermediate time scale modulation (spectral diffusion) enables vibrational echo experiments to extract dynamical information over a broad range of time scales.[22]

Appendix

The body of this paper focuses on the behavior of the overall echo decay rate. At a higher level of analysis, the echo decay shape can also be considered. Because the analysis is different from that in the body of the paper and because the results are less conclusive, this shape analysis is presented here. Despite the uncertainties in this analysis, the results indicate that the vibrational frequency modulation rates are broadly distributed and suggest directions for more detailed experiments.

For a spectral diffusion process with a simple exponential frequency−frequency correlation function, the decay of the echo signal $S_E(\tau)$ is predicted to be distinctly nonexponential[24]

$$S_E(\tau) = \exp\left[-\left(\frac{4\Gamma(1/3)\tau}{3T_E}\right)^3\right] \qquad \text{(A1)}$$

(Note that $(^1/_3)\Gamma(^1/_3) = \Gamma(^4/_3)$.) In the protein experiments, the solvent-induced contribution might follow eq A1, but the infinite-viscosity and lifetime contributions are likely to be governed by exponential decays. At low temperatures, the solvent-induced contribution is a small portion of the total decay, so the low-temperature decays will appear to be exponential even though there may be a contribution of the form given by eq A1. At high temperatures, the echo decay time is close to the pulse width. While it is possible that the shape is governed by eq A1, details of the decay shape are hard to extract. At intermediate temperatures, the solvent-induced contribution is substantial, and the decay is relatively slow. Therefore, the functional form of the solvent-induced decay can be best discerned and eq A1 can be best tested at intermediate temperatures.

The echo signal at one such intermediate temperature (220 K) is shown in Figure 6. The data are nearly linear on a semilog plot. For comparison, eq A1 is combined with an exponential decay from infinite-viscosity and lifetime contributions and a convolution due to the nonzero pulse width σ

$$S_E(\tau) = \int_0^\infty dt \left|\exp\left[-\frac{1}{2}\left(\frac{4\Gamma(1/3)t}{3T_E^r}\right)^3\right]\exp\left[-\frac{2t}{T_E(\eta=\infty)}\right]\exp\left[-\frac{(t-\tau)^2}{4\sigma^2}\right]\right|^2 \qquad \text{(A2)}$$

Because we are not trying to extract quantitative data from the pulse overlap region, the full three-time convolution has been approximated with a simpler one-time convolution. The figure shows that the shape of the fit ($T_E^r = 17$ ps, $T_E(\eta=\infty) = 21.25$ ps, and $\sigma = 0.9$ ps) is approximately correct for the first two factors of e of the decay, but overall, the fit is incompatible with the full data set.

We are left with an apparent contradiction. The analysis of the average echo decay times in section IV indicates that the solvent-driven dephasing is in the spectral-diffusion limit. In particular, the unusual $\eta^{1/3}$ behavior is characteristic of an exponential frequency−frequency correlation function in the spectral diffusion limit. In addition, the internal consistency of the physical parameters and calculated results using the viscoelastic model support the basic mechanism. However, the decay shape expected for spectral diffusion is not found. This Appendix offers a resolution of this contradiction by showing that near-exponential echo decays can occur in the presence of spectral diffusion if there is a distribution of relaxation times in the system.

At high viscosities, nonexponential relaxation (e.g., stretched exponentials, $\exp[-(t/\tau)^\beta]$)[76−78] is commonly found. In our previous paper, we looked at the case of a stretched exponential frequency−frequency correlation function in the limit of spectral diffusion and a broad inhomogeneous background process.[24] The exponent in eq A1 changes from 3 for the exponential case to $2 + \beta$ for the stretched exponential. For a reasonable value of $\beta \approx 0.5$, the echo decay shape is slightly closer to exponential but not enough to improve the fit in Figure 6 significantly. However, this result was derived assuming that the nonexponential dynamics are due to homogeneous kinetics; that is, every vibrator was assumed to experience the same stretched exponential frequency−frequency correlation function.

In general, multi-time-correlation functions, such as that governing echo spectroscopy, are sensitive to whether the kinetics are homogeneous or heterogeneous.[79] To model heterogeneous kinetics, we assume that the sample can be divided into subensembles indexed by i with different reduced echo times T_E^i. The normalized probability distribution of the echo times is given by $D(T_E^i)$. In the presence of this distribution, the echo signal averaged over the entire ensemble is

$$S_E(\tau) = \int_0^\infty \left|\int_0^\infty D(T_E^i)\exp\left[-\frac{1}{2}\left(\frac{4\Gamma(1/3)t}{3T_E^i}\right)^3\right]\exp\left(-\frac{2t}{T_E(\eta=\infty)}\right)\exp\left[-\frac{(t-\tau)^2}{4\sigma^2}\right]dT_E^i\right|^2 dt \qquad \text{(A3)}$$

The echo decay shape is strongly dependent on the form of the distribution $D(T_E^i)$. As an example, we will look at

$$D(T_E^i) = \frac{4}{T_E^0}\left(\frac{T_E^i}{T_E^0}\right)^2 \exp\left(-\frac{2T_E^i}{T_E^0}\right) \qquad \text{(A4)}$$

which has a maximum at T_E^0.

A fit using this distribution in eq A3 is shown in Figure 6 with the parameters $T_E^0 = 14.8$ ps, $T_E(\eta=\infty) = 21.25$ ps, and $\sigma = 0.9$ ps. The shape of the echo decay is reproduced almost

exactly. This fit is not unique, and we do not intend to extract quantitative results from it. However, the fit does show that an exponential echo decay can occur in the presence of spectral diffusion if the dynamics are heterogeneous.

The time extracted from the fitting procedure used in the body of the paper (17 ps) is quite close to the most probable time in this model (14.8 ps). The viscoelastic model uses a definition of the average T_E based on the integral of the decay shape.[24] For the distribution in eq A4, this definition gives $T_E = 1.19\ T_E^0$, which gives $T_E = 17.6$ ps for the data in Figure 6 (other distributions will give slightly different values). Thus, theory, experimental fits, and the heterogeneous dynamics model all use slightly different definitions of the average echo time, but in practice, these values are all very similar.

Although the distribution of echo times $D(T_E^i)$ is easiest to use in calculating the decay shape, the distribution of frequency−frequency correlation times $\tilde{D}(\tau_m^i)$ is physically more relevant. While the ensemble averaged frequency−frequency correlation function is nonexponential in this model, the correlation function for each subensemble is still exponential and fully characterized by its exponential decay time τ_m^i. The results derived in the body of the paper, for example, the $\eta^{1/3}$ dependence, applies to each subensemble and, therefore, to the ensemble average. The width of the frequency distribution Δ_m is assumed to be the same for each subensemble. Using eq 6

$$\tilde{D}(\tau_m^i) = D(T_E^i)\frac{dT_E^i}{d\tau_m} = \left(\frac{4}{3}\right)^{2/3}\frac{\Gamma(1/3)}{3(\tau_m^i\Delta_m)^{2/3}}D(T_E^i) \quad \text{(A5)}$$

in general, and

$$\tilde{D}(\tau_m^i) = \frac{1}{3\tau_m^0}\exp\left[-\left(\frac{2\tau_m^i}{\tau_m^0}\right)^{1/3}\right] \quad \text{(A6)}$$

for the example distribution, eq A4. The characteristic modulation time τ_m^i is related to the most probable echo time T_E^0 by a straightforward generalization of eq 6

$$T_E^0 = \left(\frac{4}{3}\right)^{2/3}\Gamma(1/3)\left(\frac{\tau_m^0}{\Delta_m^2}\right)^{1/3} \quad \text{(A7)}$$

Thus, the good fit to the echo decay shape in Figure 6 corresponds to a stretched exponential distribution of modulation times with $\beta = 1/3$. This fit is not unique, but any fit to the experimental decay shape will probably yield a distribution that is also very broad.

Two possible sources of dynamic heterogeneity are easy to envision. The solvent itself could have spatially distinct regions that relax with different rates. This distribution of solvent rates would then be transmitted through the protein to the CO vibration. The possibility of heterogeneous dynamics in high-viscosity liquids is currently being discussed intensely. The other possibility is that the protein is not a purely passive transmitter of the solvent relaxation at the surface, as we have assumed. There could be a lag time between changes on the protein surface and the changes experienced by the CO in the middle of the protein. If the protein adopts multiple, slowly interchanging conformational substates, and these conformations transmit surface changes to the CO at different rates, heterogeneous dynamics would result.

This appendix has shown that the echo decay shape is sensitive to the presence of heterogeneous kinetics. Comparison to experimental echo decays suggests that a broad distribution of modulation times exists in the myoglobin system. New experiments are needed that are designed to confirm the existence of this distribution, to better characterize it, and to identify its origins.

Acknowledgment. We thank Professors Alan Schwettman and Todd Smith and their students and staff at the Stanford Free Electron Laser Center for making this work possible through a grant from the Office of Naval Research (N00014-94-1-1024). We also thank Professor Dana Dlott and Dr. Jeffrey Hill at University of Illinois Urbana Champaign for providing samples and Debleena Sengupta, Department of Chemistry, Stanford University, who made the viscosity measurements. This work was supported by the National Institutes of Health under Grant 1RO1-GM61137 to M.D.F. and by the National Science Foundation under Grant CHE-9809719 to M.A.B. and Grant DMR-0088942 to M.D.F..

References and Notes

(1) Elber, R.; Karplus, M. *Science* **1987**, *235*, 318.
(2) Vitkup, D.; Ringe, D.; Petsko, G. A.; Karplus, M. *Nat. Struct. Biol.* **2000**, *7*, 34.
(3) Quillin, M. L.; Arduini, R. M.; Olson, J. S.; Phillips, G. N., Jr. *J. Mol. Biol.* **1993**, *234*, 140.
(4) Barrick, D. *Biochemistry* **1994**, *33*, 6546.
(5) Tsuda, S. *Crystallogr. Soc. Jpn.* **1996**, *38*, 84.
(6) Clore, G. M.; Gronenborn, A. M. *Prog. Nucl. Magn. Reson. Spectrosc.* **1991**, *23*, 43.
(7) Braunstein, D. P.; Chu, K.; Egeberg, K. D.; Frauenfelder, H.; Mourant, J. R.; Nienhaus, G. U.; Ormos, P.; Sligar, S. G.; Springer, B. A.; Young, R. D. *Biophys. J.* **1993**, *65*, 2447.
(8) Jackson, T. A.; Lim, M.; Anfinrud, P. A. *Chem. Phys.* **1994**, *180*, 131.
(9) Janes, S. M.; Dalickas, G. A.; Eaton, W. A.; Hochstrasser, R. M. *Biophys. J.* **1988**, *54*, 545.
(10) Oldfield, E.; Guo, K.; Augspurger, J. D.; Dykstra, C. E. *J. Am. Chem. Soc.* **1991**, *113*, 7537.
(11) Surewicz, W. K.; Mantsch, H. H. In *Spectroscopic Methods for Determining Protein Structure in Solution*; Havel, H. A., Ed.; VCH Publishers: New York, 1996; p 135.
(12) Kendrew, J. C. *Nature* **1954**, *174*, 946.
(13) Kendrew, J. C. *Nature* **1960**, *185*, 422.
(14) Stryer, L. *Biochemistry*, 3 ed.; W. H. Freeman and Co.: New York, 1988.
(15) Beece, D.; Eisenstein, L.; Frauenfelder, H.; Good, D.; Marden, M. C.; Reinisch, L.; Reynolds, A. H.; Sorensen, L. B.; Yue, K. T. *Biochemistry* **1980**, *19*, 5147.
(16) Rella, C. W.; Kwok, A.; Rector, K. D.; Hill, J. R.; Schwettmann, H. A.; Dlott, D. D.; Fayer, M. D. *Phys. Rev. Lett.* **1996**, *77*, 1648.
(17) Rector, K. D.; Rella, C. W.; Kwok, A. S.; Hill, J. R.; Sligar, S. G.; Chien, E. Y. P.; Dlott, D. D.; Fayer, M. D. *J. Phys. Chem. B* **1997**, *101*, 1468.
(18) Rector, K. D.; Engholm, J. R.; Hill, J. R.; Myers, D. J.; Hu, R.; Boxer, S. G.; Dlott, D. D.; Fayer, M. D. *J. Phys. Chem. B* **1998**, *102*, 331.
(19) Rector, K. D.; Fayer, M. D. *Int. Rev. Phys. Chem.* **1998**, *17*, 261.
(20) Rector, K. D.; Engholm, J. R.; Rella, C. W.; Hill, J. R.; Dlott, D. D.; Fayer, M. D. *J. Phys. Chem. A* **1999**, *103*, 2381.
(21) Rector, K. D.; Thompson, D. E.; Merchant, K.; Fayer, M. D. *Chem. Phys. Lett.* **2000**, *316*, 122.
(22) Leeson, D. T.; Wiersma, D. A. *Phys. Rev. Lett.* **1995**, *74*, 2138.
(23) Thijssen, H. P. H.; Dicker, A. I. M.; Völker, S. *Chem. Phys. Lett.* **1982**, *92*, 7.
(24) Berg, M. A.; Rector, K. D.; Fayer, M. D. *J. Chem. Phys.* **2000**, *113*, 3233.
(25) Loring, R. F.; Mukamel, S. *Chem. Phys. Lett.* **1985**, *114*, 426.
(26) Yan, Y. J.; Mukamel, S. *J. Chem. Phys.* **1991**, *94*, 179.
(27) Klauder, J. R.; Anderson, P. W. *Phys. Rev.* **1962**, *125*, 912.
(28) Hu, P.; Hartmann, S. R. *Phys. Rev. B* **1974**, *9*, 1.
(29) Hu, P.; Walker, L. R. *Phys. Rev. B* **1978**, *18*, 1300.
(30) Farrar, T. C.; Becker, D. E. *Pulse and Fourier Transform NMR*; Academic Press: New York, 1971.
(31) Skinner, J. L.; Anderson, H. C.; Fayer, M. D. *J. Chem. Phys.* **1981**, *75*, 3195.
(32) Levenson, M. D. *Introduction to Nonlinear Laser Spectroscopy*; Academic Press: San Jose, CA, 1982.
(33) Slichter, C. P. *Principles of Magnetic Resonance*; Springer-Verlag: Berlin, 1989.

(34) Anderson, P. W. *J. Phys. Soc. Jpn.* **1954**, *9*, 316.
(35) Kubo, R. In *Fluctuation, Relaxation and Resonance in Magnetic Systems*; Ter Haar, D., Ed.; Oliver and Boyd: London, 1961.
(36) Narasimhan, L. R.; Littau, K. A.; Pack, D. W.; Bai, Y. S.; Elschner, A.; Fayer, M. D. *Chem. Rev.* **1990**, *90*, 439.
(37) Anderson, P. W.; Halperin, B. I.; Varma, C. M. *Philos. Mag.* **1972**, *25*, 1.
(38) Phillips, W. A. *Amorphous Solids. Low-Temperature Properties, Topics in Current Physics*; Springer: Berlin, 1981.
(39) Mukamel, S. *Principles of Nonlinear Optical Spectroscopy*; Oxford University Press: New York, 1995.
(40) Berg, M.; Walsh, C. A.; Narasimhan, L. R.; Littau, K. A.; Fayer, M. D. *J. Chem. Phys.* **1988**, *88*, 1564.
(41) Ma, J.; Fourkas, J. T.; Vanden Bout, D. A.; Berg, M. In *Supercooled Liquids: Advances and Novel Applications*; Fourkas, J. T., Kivelson, D., Mohanty, U., Nelson, K. A., Eds.; American Chemical Society: Washington, DC, 1997; Vol. 676, p 199.
(42) Tokmakoff, A.; Fayer, M. D. *J. Chem. Phys.* **1995**, *103*, 2810.
(43) Rella, C. W.; Rector, K. D.; Kwok, A. S.; Hill, J. R.; Schwettman, H. A.; Dlott, D. D.; Fayer, M. D. *J. Phys. Chem.* **1996**, *100*, 15620.
(44) Angell, C. A. *J. Phys. Chem. Solids* **1988**, *49*, 863.
(45) Angell, C. A.; Smith, D. L. *J. Phys. Chem.* **1982**, *86*, 3845.
(46) Fredrickson, G. H. *Annu. Rev. Phys. Chem.* **1988**, *39*, 149.
(47) Duddu, S. P.; Dalmonte, P. R. *Pharm. Res.* **1997**, *14*, 591.
(48) Murthy, S. S. N. *J. Phys. Chem. B* **1997**, *101*, 6043.
(49) Doster, W.; Cusack, S.; Petry, W. *Phys. Rev. Lett.* **1990**, *65*, 1080.
(50) Doster, W.; Cusack, S.; Petry, W. *Nature* **1989**, *337*, 754.
(51) Loncharich, R. J.; Brooks, B. R. *J. Mol. Biol.* **1990**, *215*, 439.
(52) Steinbach, P. J.; Brooks, B. R. *Proc. Natl. Acad. Sci. U.S.A.* **1993**, *90*, 9135.
(53) Hong, M. K.; Draunstein, D.; Cowen, B. R.; Frauenfelder, H.; Iben, I. E. T.; Mourant, J. R.; Ormos, P.; Scholl, R.; Schulte, A.; Steinbach, P. J.; Xie, A.; Young, R. D. *Biophys. J.* **1990**, *58*, 429.
(54) Mayer, E. *Biophys. J.* **1994**, *67*, 862.
(55) Cordone, L.; Cupane, A.; Leone, M.; Vitrano, E. *J. Mol. Biol.* **1988**, *199*, 213.
(56) Parak, F.; Knapp, E. W.; Kucheida, D. *J. Mol. Biol.* **1982**, *161*, 177.
(57) Oldfield, E.; Guo, K.; Augspurger, J. D.; Dykstra, C. E. *J. Am. Chem. Soc.* **1991**, *113*, 7537.
(58) Augspurger, J. D.; Dykstra, C. E.; Oldfield, E. *J. Am. Chem. Soc.* **1991**, *113*, 2447.
(59) Park, E.; Andrews, S.; Boxer, S. G. *J. Phys. Chem. B* **1999**, *103*, 9813.
(60) Hill, J. R.; Dlott, D. D.; Rella, C. W.; Peterson, K. A.; Decatur, S. M.; Boxer, S. G.; Fayer, M. D. *J. Phys. Chem.* **1996**, *100*, 12100.
(61) Hill, J. R.; Dlott, D. D.; Fayer, M. D.; Rella, C. W.; Rosenblatt, M. M.; Suslick, K. S.; Ziegler, C. J. *J. Phys. Chem.* **1996**, *100*, 218.
(62) Hill, J. R.; Rosenblatt, M. M.; Ziegler, C. J.; Suslick, K. S.; Dlott, D. D.; Rella, C. W.; Fayer, M. D. *J. Phys. Chem.* **1996**, *100*, 18023.
(63) Cooper, A. *Proc. Natl. Acad. Sci. U.S.A.* **1976**, *73*, 2740.
(64) Rector, K. D.; Zimdars, D. A.; Fayer, M. D. *J. Chem. Phys.* **1998**, *109*, 5455.
(65) Berg, M. A.; Hubble, H. W. *Chem. Phys.* **1998**, *233*, 257.
(66) Berg, M. *J. Phys. Chem. A* **1998**, *102*, 17.
(67) Berg, M. A. *J. Chem. Phys.* **1999**, *110*, 8577.
(68) Hubble, H. W.; Lai, T.; Berg, M. A. *J. Chem. Phys.*, in press.
(69) Zwanzig, R.; Mountain, R. D. *J. Chem. Phys.* **1965**, *43*, 4464.
(70) Bertolini, D.; Tani, A. *Phys. Rev. E* **1995**, *52*, 1699.
(71) Piccirelli, R.; Litovitz, T. A. *J. Acoust. Soc. Am.* **1957**, *29*, 1009.
(72) Jiang, J.; Berg, M. A. Unpublished results.
(73) Litovitz, T. A.; Davis, D. M. In *Physical Acoustics*; Mason, W. P., Ed.; Academic Press: New York, 1965; Vol. IIA.
(74) Harrison, G. *The Dynamic Properties of Supercooled Liquids*; Academic Press: New York, 1976.
(75) Forrest, J. A.; Dalnoki-Veress, K.; Dutcher, J. R. *Phys. Rev. E* **1997**, *56*, 5705.
(76) Cummins, H. Z.; Li, G.; Du, W.; Hwang, Y. H.; Shen, G. Q. *Prog. Theor. Phys. Suppl.* **1997**, *126*, 21.
(77) Fuchs, M.; Hofacker, I.; Latz, A. *Phys. Rev. A* **1992**, *45*, 898.
(78) van Megen, W.; Underwood, S. M. *Phys. Rev. E* **1994**, *49*, 4206.
(79) Heuer, A. *Phys. Rev. E* **1997**, *56*, 730.